Composites Part B 127 (2017) 150–165

Contents lists available at ScienceDirect

Composites Part B

journal homepage: www.elsevier.com/locate/compositesb

Bond between TRM versus FRP composites and concrete at high temperatures

Saad M. Raoof [a, b, *], Dionysios A. Bournas [c]

[a] Department of Civil Engineering, University of Nottingham, NG7 2RD, Nottingham, UK
[b] Department of Civil Engineering, University of Tikrit, Tikrit, Iraq
[c] European Commission, Joint Research Centre (JRC), Directorate for Space, Security and Migration, Safety and Security of Buildings Unit, via E. Fermi 2749, I-21027 Ispra, Italy

ARTICLE INFO

Article history:
Received 4 February 2017
Received in revised form
7 April 2017
Accepted 21 May 2017
Available online 25 May 2017

Keywords:
Fabrics/textiles
Carbon fibre
Debonding
High temperature

ABSTRACT

The use of fibre reinforced polymers (FRP) as a means of external reinforcement for strengthening the existing reinforced concrete (RC) structures nowadays is the most common technique. However, the use of epoxy resins limits the effectiveness of FRP technique, and therefore, unless protective (thermal insulation) systems are provided, the bond capacity at the FRP-concrete interface will be extremely low above the glass transition temperature (T_g). To address problems associated with epoxies and to provide cost-effectiveness and durability of the strengthening intervention, a new composite cement- based material, namely textile-reinforced mortar (TRM) has been developed the last decade. This paper for the first time examines the bond performance between the TRM and concrete interfaces at high temperatures and, also compares for the first time the bond of both FRP and TRM systems to concrete at ambient and high temperatures. The key parameters investigated include: (a) the matrix used to impregnate the fibres, namely resin or mortar, resulting in two strengthening systems (TRM or FRP), (b) the level of high temperature to which the specimens are exposed (20, 50, 75, 100, and 150 °C) for FRP-reinforced specimens, and (20, 50, 75, 100, 150, 200, 300, 400, and 500 °C) for TRM-strengthened specimens, (c) the number of FRP/TRM layers (3 and 4), and (d) the loading conditions (steady state and transient conditions). A total of 68 specimens (56 specimens tested in steady state condition, and 12 specimens tested in transient condition) were constructed, strengthened and tested under double- lap direct shear. The result showed that overall TRM exhibited excellent performance at high temperature. In steady state tests, TRM specimens maintained an average of 85% of their ambient bond strength up to 400 °C, whereas the corresponding value for FRP specimens was only 17% at 150 °C. In transient test condition, TRM also outperformed over FRP in terms of both the time they maintained the applied load and the temperature reached before failure.

1. Introduction and background

There is a growing need for upgrading the existing reinforced concrete (RC) structures both in seismic and non-seismic areas. This is attributed to deterioration of RC structures as a result of ageing, inadequate maintenance, environmental induced degradation but also due to the increase of the applied loads and the need to comply with the modern standards (for example Eurocodes) requirements.

The use of Fibre-Reinforced Polymer (FRP) as external strengthening system has gained high popularity among other techniques. This is due to the favorable properties offered by FRP such as resistance to corrosion, high strength to weight ratio, ease and speed of application and minimal change in the geometry. However, due to the epoxy resins used in these composites, the FRP systems are usually expensive, cannot be applied at low temperatures or wet surfaces, are combustible and could boost fire spreading and have very poor performance at high temperature, as under loading epoxy resins normally lose their tensile capacity. Therefore, unless protective (thermal insulation) systems are not provided [1], the bond strength between the FRP and concrete substrate will be extremely low above the glass transition

* Corresponding author. Department of Civil Engineering, University of Nottingham, NG7 2RD, Nottingham, UK.
E-mail addresses: Saad.Raoof@nottingahm.ac.uk (S.M. Raoof), dionysios.bournas@ec.europa.eu (D.A. Bournas).

http://dx.doi.org/10.1016/j.compositesb.2017.05.064

temperature (T_g). A review on the behaviour RC members strengthened with FRPs and subjected to fire or high temperature was recently conducted by Firmo et al. [2].

To address the problems of FRP, a novel composite material called textile-reinforced mortar (TRM) has been introduced since last decade, for structural strengthening of existing structures [3]. TRM consists of textile fibre reinforcement (with open-mesh configuration) combined with inorganic matrices (i.e. cementitious mortars). The acronym 'TRC' [4] or 'FRCM' [5] is also used in the literature for the same material. TRM is a low-cost, resistant at high temperature, compatible to masonry or concrete substrates and friendly for manual workers material, which can be applied at low temperatures or on wet surfaces. Therefore, the use of TRM is becoming more attractive for the retrofitting of existing concrete or masonry structures than FRP. A number of studies have demonstrated that TRM is an effective technique for the flexural strengthening of beams [i.e. [6–9]], one way [i.e. [10, 11]], and two way slabs [12]; the shear upgrading of RC beams [i.e. [13, 14]]; the seismic retrofitting of RC columns (e.g. Refs. [15–20]); and the seismic retrofitting of infilled RC frames [21].

The effectiveness of externally bonded FRP or TRM systems depends primarily on the bond at the composite-concrete interface. At high temperatures or in case of a fire, the bond between FRP and concrete becomes negligible, reducing dramatically the performance of the FRP technique. The bond between FRP and concrete at high temperature has been addressed in Refs. [22–25]; in these studies, double-lap direct shear tests were conducted on concrete blocks externally strengthened with Carbon fibre reinforced polymers (CFRP). The specimens were exposed to a predefined temperature varied between 20 and 120 °C and then tested up to failure. It was demonstrated that the bond between FRP materials and concrete significantly deteriorated when the temperature of adhesive is equal or above T_g.

TRM could outperform FRP systems at high temperatures or fire due to the breathability, non-combustibility, and non- flammability offered by mineral-based cement mortars used as binding materials. Until now, the bond between TRM materials and concrete substrate has been addressed only at ambient temperatures [i.e. [26–28]] and no single study exists at high temperatures or fire. In general, the research on the performance of TRM systems at elevated temperature or fire and the comparison between TRM and FRP systems at high temperature or fire is extremely limited [29–33]. This is attributed to the inherent experimental difficulties applying simultaneously loading and high temperature, even for medium or small-scale specimens. For this reason, the past studies mainly evaluated the residual strength of TRM after being exposed to high temperatures and cooled down to the ambient temperature. Particularly in Refs. [29–31] uniaxial tensile tests were conducted on TRM coupons made of glass [29], carbon [30], and basalt [31] textile fibres. The test procedure included the following steps: (a) exposure to elevated temperatures of 20, 200, 400, and 600 °C [29]; 20, 100, 150, 200, 400, and 600 °C [30]; and 20, 75, 150, 200, 300, 400, 600, and 1000 °C [31]; (b) exposing the specimens at these temperatures for: 2 h [29], 3 h [30], and 1 h [31] (stabilizing phase); (c) cooling down the specimens to the ambient temperature; and (d) conducting a uniaxial tensile test up to failure. The main conclusion of these studies was that TRM coupons maintained their ambient tensile strength at high temperature up to 200 °C [29,30], and 150 °C [31]. However, above these temperatures, the residual tensile strength was gradually decreased due to the deterioration of tensile strength of the textile fibres themselves.

The only studies reported in the literature on TRM versus FRP as strengthening materials at high temperature is that of Bisby et al. [32] and Tetta and Bournas [33], who did flexural and shear strengthening of RC beams, respectively. In Ref. [32], a sustained load was applied on medium-scale beams, and then the temperature was increased (except from anchorage zones where they kept cold) up to failure. In Ref. [33], medium and full-scale beams were heated up to predefined temperature (20, 100, 150 and 250 °C) and then loaded monotonically up to failure. In Ref. [32], it was concluded that both strengthening systems (TRM and FRP) can have the same performance at high temperature if the anchorage zones of the beams kept cold. Whereas, in Ref. [33] it was found that TRM exhibited superior performance over FRP at high temperature where the effectiveness of the latter dropped to about zero when the temperature at the concrete/adhesive reached T_g.

This paper investigates experimentally, for the first time the bond between TRM and concrete substrates at high temperatures. Furthermore, it compares for the first time the bond strength of TRM vs FRP with concrete substrates at different elevated temperatures and loading conditions. The investigated parameters include: (a) the number of layers (three and four layers); (b) the elevated temperatures (20, 50, 75, 100 and 150 °C for FRP strengthened specimens and 20, 50, 75, 100, 150, 200, 300, 400 and 500 °C for TRM strengthened specimens) and; (c) the loading condition (steady-state and transient conditions).

2. Experimental programme

2.1. Test specimens and investigated parameters

The main aim of this study was to compare the bond of two strengthening systems namely, FRP and TRM with concrete at different elevated temperatures and loading conditions. In total 68 specimens (34 twin specimens as a measure to reduce the scatter of the results) were constructed, strengthened and tested under direct tensile test. The details of the specimens are provided in Fig. 1a–f. Each specimen comprised two RC prisms with dimensions of 100 × 100 mm cross section and 265 mm length. The two prisms were connected only by FRP/TRM layers which were bonded on two opposite sides of the prisms.

The procedure for specimen's preparation was as follows: an acrylic plate with dimensions of 100 × 100 mm cross sectional was fixed at the middle of a steel mould (Fig. 1a) in order to isolate the two prisms during casting stage. The acrylic plate provided with two acrylic rods with 10-mm diameter fixed at the position shown in Fig. 1b so as to create holes into concrete mass of each prism. Each prism was reinforced with a steel cage with the details shown in Fig. 1c to prevent the failure of prisms due to concrete splitting during the test. A 16-mm bar was fitted at the centre of each prism in order to allow for the application of the load during the test (Fig. 1 d). After 24 h of casting, the specimen (two prisms) was removed from the mould, the acrylic plate was remove from the central zone, and the two prisms were reconnected to each other's using a 10-mm diameter aluminium rods (Fig. 1d) that were inserted into the premade holes (Fig. 1d). The purpose of these two aluminium rods was to ensure fully alignment between the two prisms and reduce the error in the measurements resulted from the possible bending of specimen due to misalignment between the two prisms. Finally, full details about the design of test specimen including a free body diagram of the tested side of the specimen are provided in Fig. 1e and f, respectively.

A number of parameters were investigated in this study comprising: (a) the matrix used to impregnate the fibres, namely resin or mortar, resulting in two strengthening systems (TRM or FRP), (b) the temperature to which the specimens were exposed (50, 75, 100, 150 °C) for FRP and (50, 75, 100, 150, 200, 300, 400 and 500 °C) for TRM retrofitted specimens (c) the number of layers (3 and 4), and (d) the loading condition, namely steady state test and transient test conditions. In the steady state test, 28 twin specimens

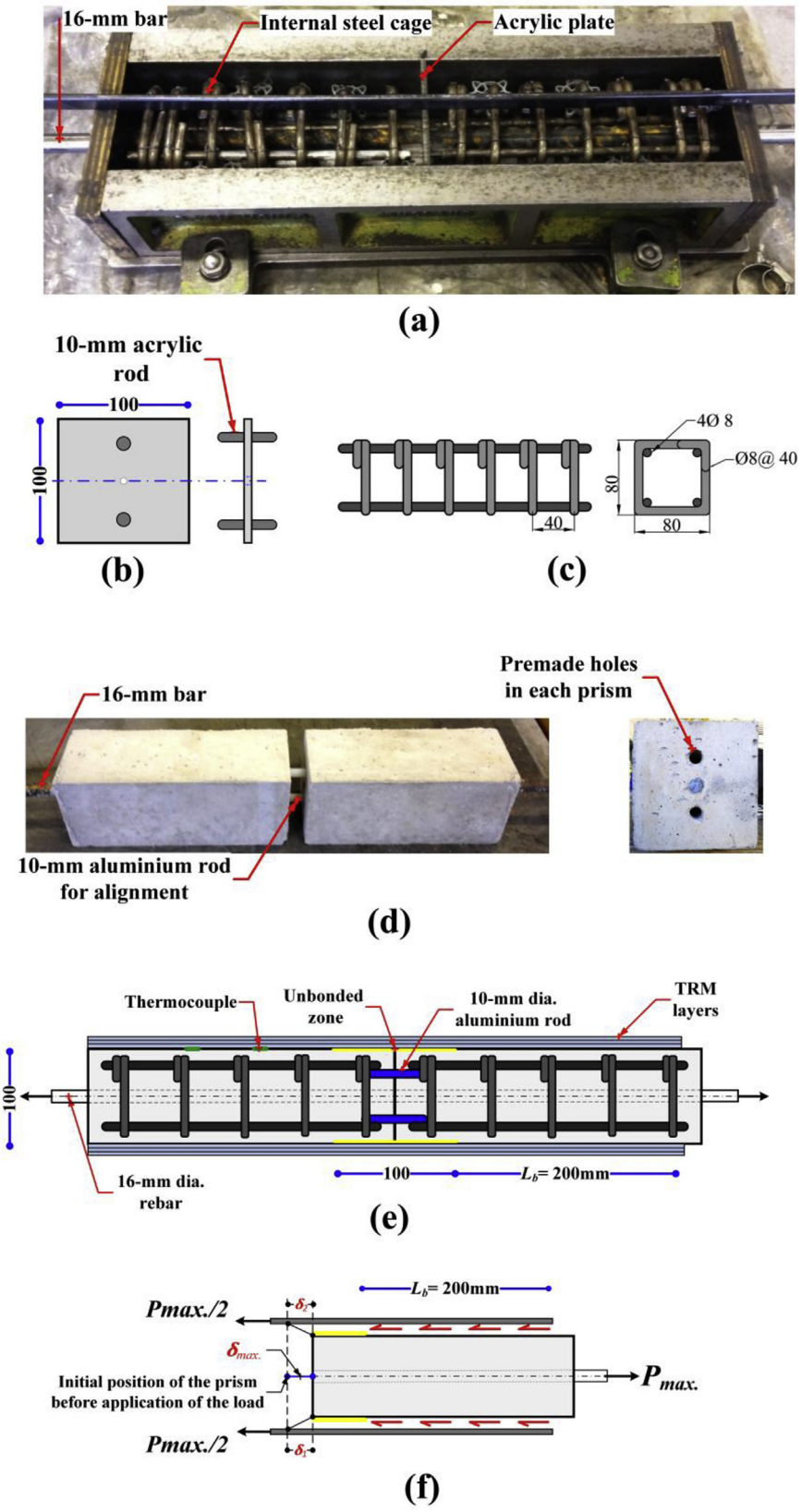

Fig. 1. Specimen details; (a) specimen preparation; (b) details of acrylic plate; (c) details of internal reinforcement; (d) details of alignment of the prisms; (e) overall design details of the test specimen; and (f) schematic diagram for the free body diagram of the tested side of the specimen (Dimensions in mm).

Table 1
Specimens details, concrete compressive strength, and mortar properties on the day of testing.

Specimen	Temp. (°C)	Number of layers	Concrete compressive strength (MPa)	Mortar	
				Flexural strength (MPa)*	Compressive strength (MPa)*
M3_20[a]	Ambient	3	33.7 (0.8)*	9.9 (0.3)*	39.9 (2.1)*
M3_50	50	3		3.93 (0.07)*	20.8(2.2)*
M3_75	75	3		3.49 (0.35)*	19.1(1.9)*
M3_100	100	3		2.35 (0.12)*	14.5(1.6)*
M3_150	150	3		2.2 (0.18)*	14.1(0.9)*
M3_200	200	3		2.3 (0.19)*	15.2 (1.2)*
M3_300	300	3		3.31 (0.05)*	19.8(0.8)*
M3_400	400	3		3.73 (0.08)*	21.9(2.7)*
M3_500	500	3		1.31 (018)*	12.7(0.6)*
M4_20[a]	Ambient	4	31.4 (2.3)*	10.6 (1)*	40.9 (2.5)*
M4_50	50	4		3.93 (0.07)*	20.8(2.2)*
M4_75	75	4		3.49 (0.35)*	19.1(1.9)*
M4_100	100	4		2.35 (0.12)*	14.5(1.6)*
M4_150	150	4		2.2 (0.18)*	14.1(0.9)*
M4_200	200	4		2.3 (0.19)*	15.2 (1.2)*
M4_300	300	4		3.31 (0.05)*	19.8(0.8)*
M4_400	400	4		3.73 (0.08)*	21.9(2.7)*
M4_500	500	4		1.31 (018)*	12.7(0.6)*
R3_20	Ambient	3	32.8 (1.6)*	–	–
R3_50	50	3		–	–
R3_75	75	3		–	–
R3_100	100	3		–	–
R3_150	150	3		–	–
R4_20	Ambient	4	29.7 (1.1)*	–	–
R4_50	50	4		–	–
R4_75	75	4		–	–
R4_100	100	4		–	–
R4_150	150	4		–	–

*Standard deviation in parenthesis.
[a] Specimens included in Raoof et al. 2016 [28].

were heated up to a predefined temperature (see Table 1), kept at this temperature for 60 min, and then loaded monotonically up to failure. In the transient test, 12 twin specimens were first loaded (at ambient temperature) up to a load fraction equal to 25%, 50%, and75% of the bond strength of the corresponding specimens tested at ambient temperature and then the specimens were heated up to failure.

The specimens' notation is BN_T, where B represents the type of bonding agent (R for epoxy resin and M for cement mortar), N

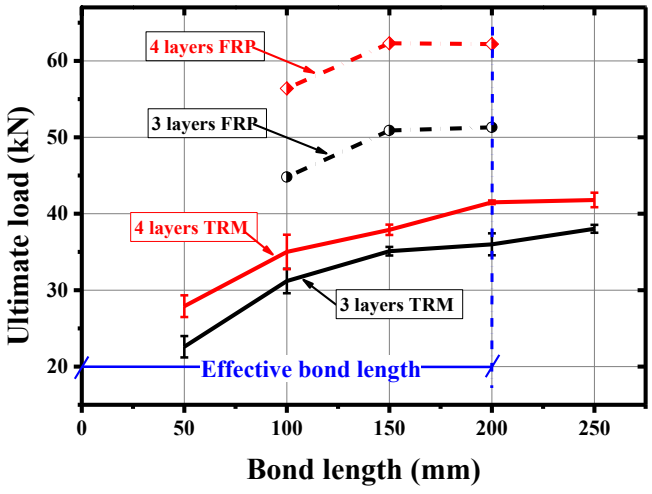

Fig. 2. Variation of ultimate load with the number of layers and the bond length for both strengthening systems; the results of TRM system have already been presented in Ref. [28].

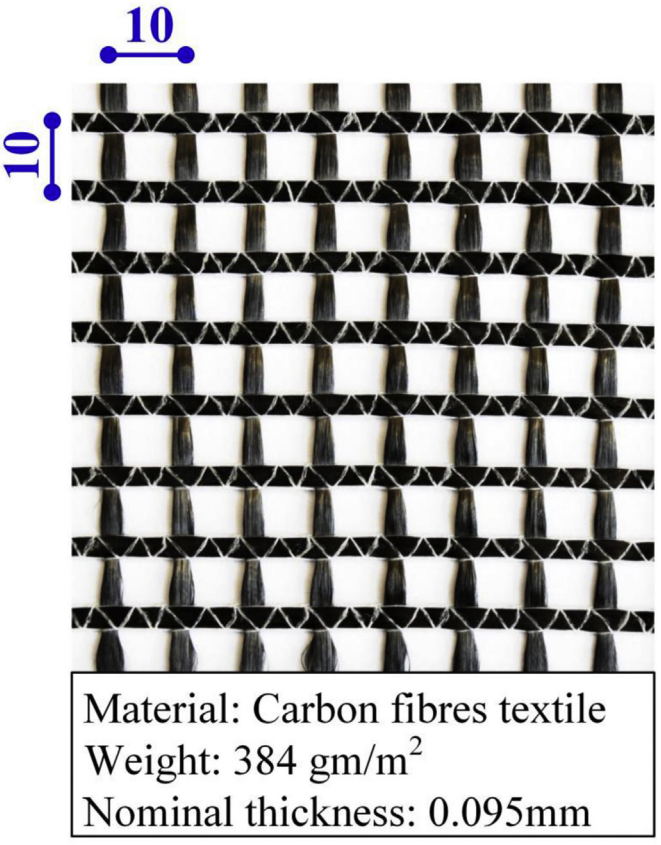

Fig. 3. Carbon fibre textile used in this study.

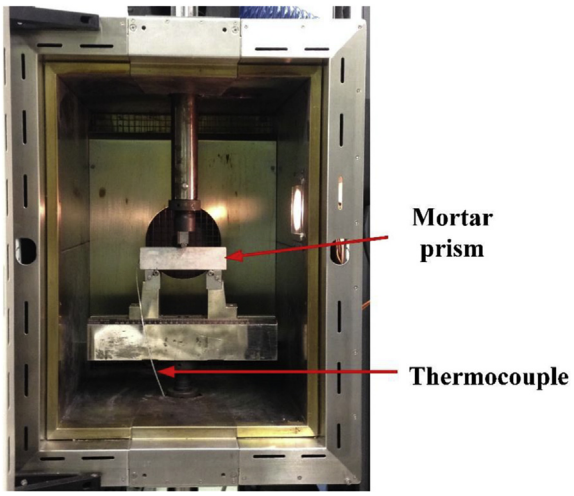

Fig. 4. Test setup for the mortar prisms tested at high temperature.

refers to the number of FRP/TRM layers, whereas T denotes the exposed temperature for steady state tests, and the loading fraction of specimens tested at ambient for transient test condition. For example, M4_400 refers to a specimen strengthened with 4 TRM layers and tested monotonically (in steady state condition) at 400 °C; whereas, M4_75% denotes to a 4 layers TRM specimen, subjected to a load fraction of 75% of the bond strength measured at ambient temperature, and then exposed to high temperature up to failure. Details for each parameter of all specimens are presented in Table 1.

Note that the bond length of FRP/TRM reinforcement was the same and equal to 200 mm for all tested specimens (see Fig. 1e). This length was selected on the basis a previous study of the authors [28], where it was found that the effective bond length (for 3–4 strengthening carbon layers) was approximately equal to 200 mm and 150 mm for the TRM and FRP systems, respectively, as illustrated in Fig. 2.

2.2. Materials and strengthening procedure

The specimens were cast in different groups using the same mix design. The concrete compressive strength was obtained on the day of the testing. Table 1 reports the value of the concrete compressive strength (average of three 150 mm cubes).

A high strength carbon fibres textile was used as an external reinforcement which comprised equal quantity of rovings in both in the two orthogonal directions. The mesh size, the weight, and the nominal thickness is illustrated in Fig. 3. It is noted that the nominal thickness was calculated based on the equivalent smeared distribution of fibres. Uniaxial tensile tests were conducted on coupons made of bare carbon fibres textile in order to determine its tensile behaviour in the loading direction. The average calculated tensile strength, ultimate strain, and modulus of elasticity were 1518 MPa, 0.911%, and 166.8 GPa, respectively.

For the specimens that received TRM as strengthening materials, an inorganic modified cement mortar was used as a bonding agent. This cement mortar was consisted of cement and polymers. The ratio of cement to polymers was 8:1 by weight. The water-cement ratio of the mortar was 0.23:1 by weight. This ratio resulted in a mortar with a good workability and plastic consistency. The compressive and flexural strength of the cement mortar both at

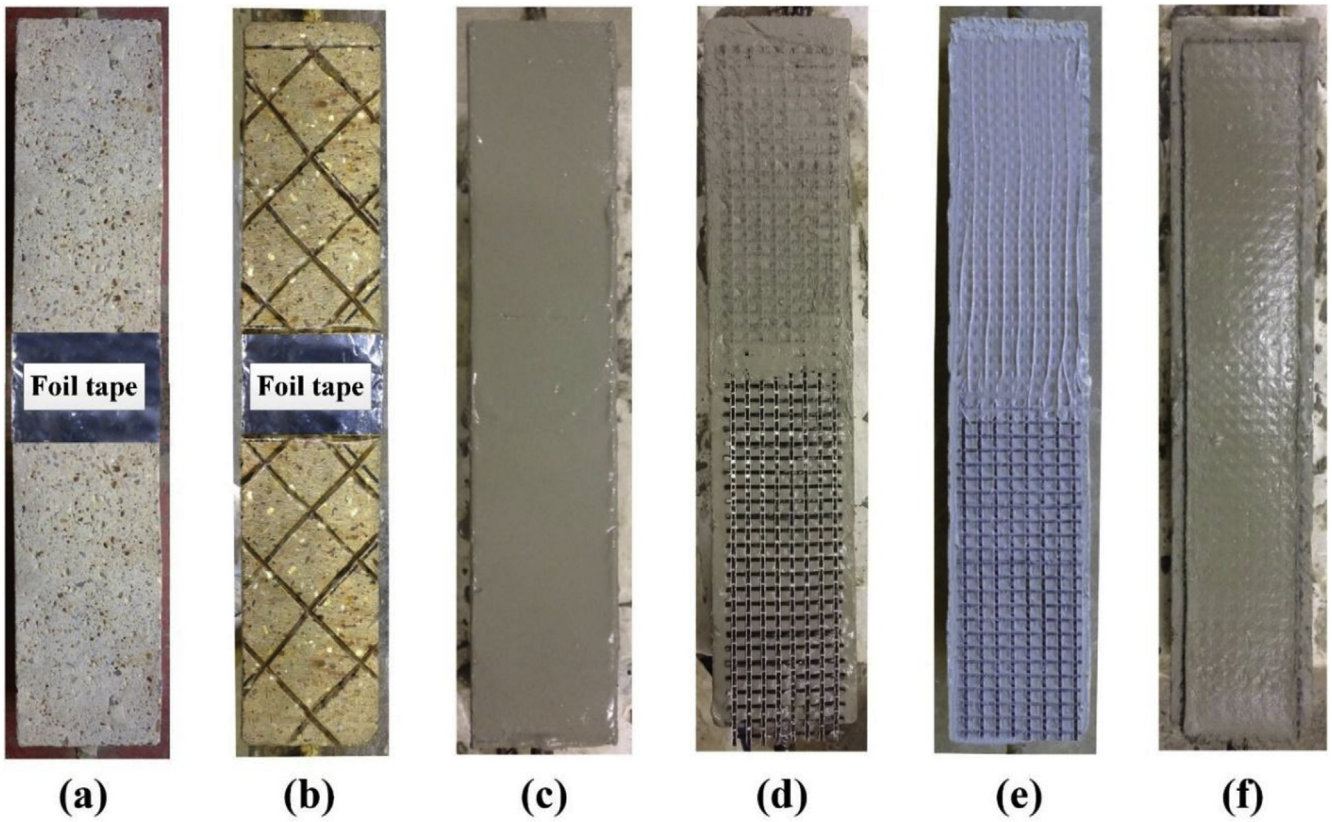

Fig. 5. Strengthening procedure: (a) surface preparation for TRM strengthened specimens; (b) surface preparation for FRP strengthened specimens; (c) application of the first of mortar; (d) application of the first layer of textile for TRM retrofitted specimens; (e) application of first layer of textile for FRP retrofitted specimens; and (f) application of final layer of mortar for TRM retrofitted specimens.

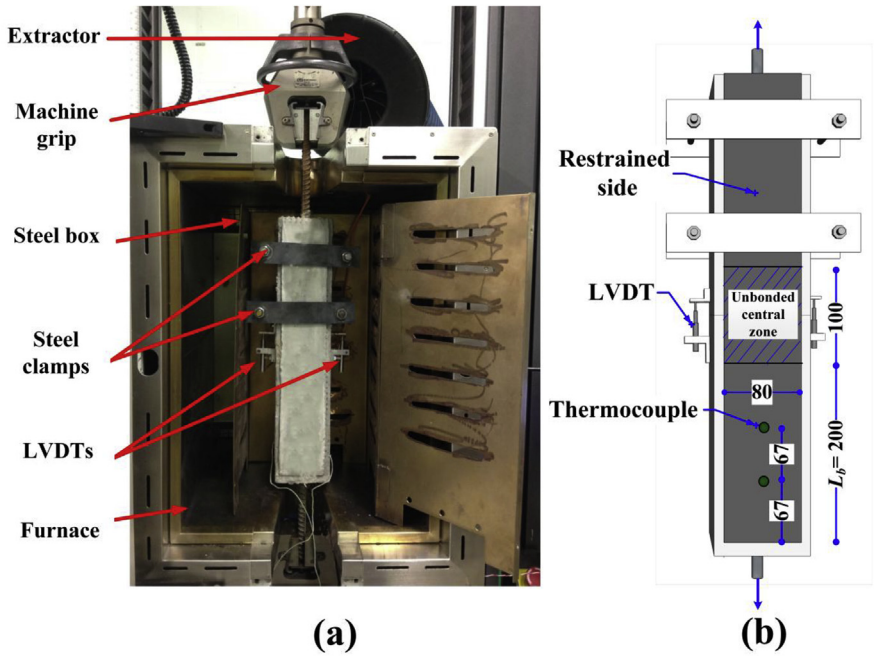

Fig. 6. (a) Details of the test setup; (b) details of test specimen.

ambient and high temperature were experimentally obtained on the day of testing. Three mortar prisms with dimensions of 40 × 40 × 160 mm were used to determine the compressive and flexural strength. The prisms were fixed in the furnace as shown in Fig. 4, heated up to the desired temperature, kept for 1 h at this temperature, and then tested according to the EN 1015-22 specifications [34]. Table 1 reports the results of compressive and flexural strength of the mortar prisms (average value from 3 prisms). For the specimens retrofitted with FRP, an epoxy resin comprising two-part with a mixing ratio of 4:1 by weight was used. The tensile strength, the modulus of elasticity, and the T_g of the epoxy resin were 30 MPa, 3.8 GPa, and 68 °C, respectively, according to the manufacturer datasheets.

The strengthening procedure for both strengthening systems had the characteristics of a typical wet lay-up application and comprised the following steps:

- Prior to the application of the strengthening materials (TRM or FRP), the concrete surface was prepared as follows: (a) for FRP-strengthened specimens, a thin layer of the concrete cover was removed followed by roughening the surface, and the resulted concrete surface was cleaned from dust (Fig. 5a); (b) for TRM-strengthened specimens, after removing the thin layer of concrete, a 50-mm mesh of grooves with a depth of approximately 2–3 mm was created. Then, the resulted surface was cleaned with compressed air, followed by dampening with water before applying the strengthening (Fig. 5b).
- Before application of strengthening materials, a 100 mm-long central zone was wrapped with a foil tape (Fig. 5 a, b) in order to isolate the strengthening materials from the concrete prisms at this zone and prevent any possible attachment with the concrete surface.
- For TRM-retrofitted specimens, the first mortar layer (approximately 2 mm-thick) was applied (Fig. 5c); followed by the application of the first layer of textile. (Fig. 5d). For specimens that received FRP, the first layer of the textile fibres was applied on a thin layer of epoxy resin and impregnated using a plastic roll (Fig. 5e).
- The above procedure was repeated until the required number of layers (3 or 4 layers) was applied.
- Finally, for the specimens retrofitted with TRM, the last textile layer was covered and levelled with an external layer of mortar (Fig. 5f).

2.3. Test setup, instrumentation and procedure

The specimens were positioned inside a furnace with inner chamber dimensions of 600 mm × 400 mm x 400 mm and maximum temperature capacity of 600 °C. The furnace was installed into a universal testing machine of 250 kN capacity, as shown in Fig. 6a. The instrumentations used for specimens tested in steady state condition included: (i) Two high temperature LVDTs, fixed to the specimens' un-strengthened sides to measure the relative displacement between the two prisms (Fig. 6a and b); (ii) two thermocouples type-K with diameter of 1.2 mm, fixed at the

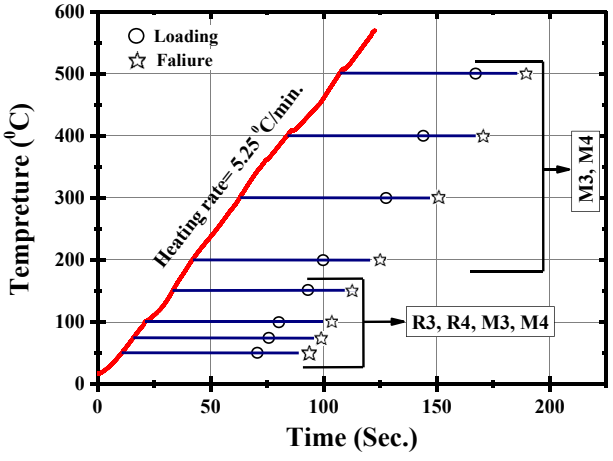

Fig. 7. Scheme of time- temperature curve.

matrix- concrete interface and located at the positions shown in Figs. 1e and 6b to monitor the temperature at this interface; (iii) Five high temperature strain gages were mounted to the surface of TRM along the tested bond length to measure the strain distribution. Two steel clamps were fixed to the not-instrumented side of the specimens as shown in Fig. 6a and b. The purpose of these clamps was to prevent the failure in the un-instrumented side and ensure that the failure would occur in the instrumented side. As can also be observed in Fig. 6a, the specimen was encased in a steel box to protect the furnace in case of explosion.

For specimens tested in steady state condition the following steps were adopted: (a) positioning of the specimens inside the furnace and fixing only to the upper grip of the testing machine (Fig. 6a); (b) heating up to the predefined target temperature described in Table 1, with an average heating rate of 5.25 °C/min, and keeping the target temperature constant for 60 min (Fig. 7); (c) fixing the lower grip of the testing machine; and (d) monotonic loading up to failure, under displacement control with a rate of 0.2 mm/min.

For specimens tested in transient condition, the following procedure was carried out: (a) positioning in the furnace (at ambient temperature) and fixing to the machine grips; (b) loading up to the targeted load fraction of 25%, 50%, and 75% of the average ultimate load recorded for the specimens tested at ambient temperature; (c)

Table 2
Summary of test results.

Specimen	(1) Maximum load, $P_{max.}$ (kN)		(2) Displacement at maximum load $??_{max}$ (mm)		(3) Average maximum load, $P_{av.}$ (kN)	(4) Average displacement at maximum load $??_{av}$ (mm)	(5) $P^{H.T.}_{max}/P^{A.T.}_{max}$	(6) Average bond strength (MPa)	(7) Average tensile stress in the textile (MPa)	(8) Failure mode[b]
	S1[a]	S2[a]	S1[a]	S2[a]						
R3_20	52.2	50.4	0.52	0.69	51.3	0.61	–	1.60	1125	D
R3_50	30.9	29	0.6	0.78	30.0	0.69	0.58	0.94	657	
R3_75	18.2	17.5	0.44	0.57	17.9	0.51	0.35	0.56	391	A
R3_100	15.8	13.5	0.53	0.68	14.7	0.61	0.28	0.46	3121	
R3_150	9.4	8.7	0.23	0.37	9.1	0.30	0.18	0.28	198	
R4_20	63.2	61.1	0.77	1.1	62.2	0.94	–	1.94	1022	D
R4_50	42.4	38.8	0.76	0.88	40.6	0.82	0.65	1.27	668	
R4_75	24.3	20.8	0.53	0.42	22.6	0.48	0.36	0.70	371	A
R4_100	16.7	14.8	0.5	0.67	15.8	0.59	0.25	0.49	259	
R4_150	10.4	9.1	0.37	0.51	9.8	0.44	0.16	0.30	160	
M3_20[c]	37.4	34.6	1.57	1.9	36.0	1.74	–	1.13	789	D
M3_50	29.0	29.6	0.75	0.99	29.3	0.87	0.81	0.92	643	D
M3_75	28.9	24	1.29	1.1	26.5	1.20	0.73	0.83	580	
M3_100	29.8	29.0	1.3	1.04	29.4	1.17	0.82	0.92	645	
M3_150	29.1	32.7	1.1	1.33	30.9	1.22	0.86	0.97	678	
M3_200	27.2	25.1	1.35	1.56	26.2	1.46	0.73	0.82	573	
M3_300	33.8	38	1.79	1.46	35.9	1.63	1.00	1.12	787	
M3_400	33.2	37.6	1.84	1.55	35.4	1.70	0.98	1.11	776	
M3_500	16.6	19.2	0.7	0.78	17.9	0.74	0.50	0.56	393	
M4_20[c]	41.7	41.3	1.57	1.31	41.5	1.44	–	1.30	683	D
M4_50	36.7	31.3	1.14	1.39	34.0	1.27	0.82	1.06	559	D
M4_75	32.3	36.4	1.02	0.85	34.4	0.94	0.83	1.07	565	
M4_100	36.2	36.2	1.28	1.25	36.2	1.27	0.87	1.13	595	
M4_150	36.9	36.1	1.17	1.26	36.5	1.22	0.88	1.14	600	
M4_200	38.5	35.2	1.44	1.05	36.9	1.25	0.89	1.15	606	
M4_300	36.5	41.2	1.46	1.18	38.9	1.32	0.94	1.21	639	
M4_400	37.6	40.7	1.72	1.43	39.2	1.58	0.94	1.22	644	
M4_500	21.8	24.3	0.75	0.87	23.1	0.81	0.56	0.72	379	

[a] Specimen number.
[b] D: Debonding of FRP/TRM from the concrete substrate including part of the concrete cover; A: Adhesive failure at the concrete-resin interface.
[c] Specimens included in Raoof et al., 2016 [28].

Table 3
Results of transient condition test.

Specimen	(1) Load (kN)	(2) Time (min.)		(3) Average time (min.)	(4) Temperature (°C)		(5) Average temperature (°C)	(6) Failure mode[b]
		S1[a]	S2[a]		S1[a]	S2[a]		
R4_25%	15.5	19.9	18	19.0	100.8	91.8	96.3	A
R4_50%	31.1	16.3	17.7	17.0	66.4	74.9	70.7	D
R4_75%	46.6	11.9	12.7	12.3	47.5	50.2	48.9	D
M4_25%	10.4	65.6	58.3	62.0	329.8	309.2	319.5	D
M4_50%	20.8	62.3	55.2	58.8	319.6	301.1	310.4	D
M4_75%	31.1	18	21	19.5	72.4	82.2	77.3	D

[a] Specimen number.
[b] A: dhesive failure a the concrete-resin interface (see Fig. 15a); D: Debonding of FRP/TRM from the concrete substrate with peeling off part of the concrete cover (see Fig. 15 b and c for FRP specimens and Fig. 15 d–f for TRM specimens).

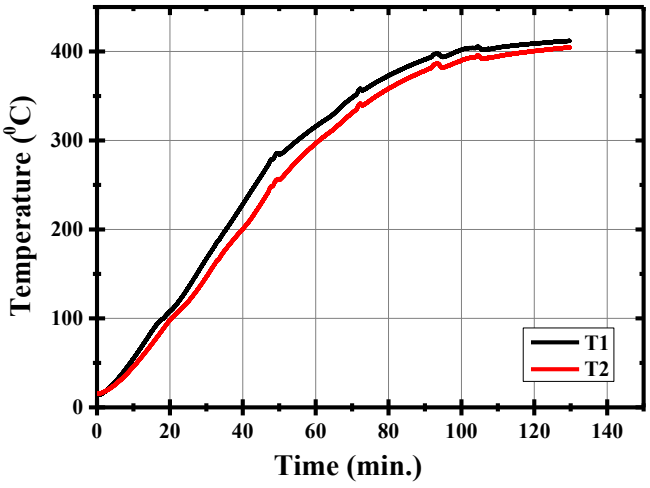

Fig. 8. Time- temperature curve obtained from the two thermocouples for a specimen tested in steady state and heated up to 400 °C.

heating the specimens with the same heating rate (5.25 °C/min) up to failure. An extractor was used to remove the smoke if was released as a result of heating the specimens up.

Finally, it is worth mentioning that the FRP/TRM reinforcement was left un-bonded at 100 mm-long central zone (50 mm at each prism) of the specimen (Fig. 6b) to prevent from edge failure of the concrete prisms. Furthermore, the bond width of FRP/TRM reinforcement was the same for all tested specimens and was equal to 80 mm s (see Fig. 6b).

3. Experimental results

Fig. 1f shows the free body diagram of the tested side of the specimen. By assuming perfect symmetry of the specimen (up to peak load), the interface between the FRP/TRM strip and concrete in each side of the tested part will carry half of the measured ultimate load ($P_{max.}$). The relative displacement between the two concrete prisms measured at ultimate load will be the average of the two LVDTs' readings; $\delta_{max} = (\delta 1 + \delta 2)/2$.

The main experiment results of all specimens tested in both loading conditions are presented in Tables 2 and 3. Table 2, reports the results of the steady state test including: (1) the ultimate load (P_{max}) recorded for twin specimens S1 and S2; (2) the relative displacement ($\delta_{max.}$). recorded at the ultimate load (P_{max}); (3) the value of average load (P_{av}) of the twin specimens; (4) the average displacement (δ_{av}) of the twin specimens; (5) the ratio of high to ambient temperature bond strength, expressed as $P^{H.T.}_{max}/P^{A.T.}_{max}$ to quantify the effect of high temperatures on the bond strength; (6) the average bond strength developed at the concrete-adhesive interface, calculated as $(P_{av}/2)/Lb$, (7) the average tensile stress (σ_t) developed in the textile, calculated as $(P_{av}/2)/ntb$, and (8) the observed failure mode. Where L, and b is the bond length and width ($L = 200$, and b = 80 mm), respectively, n is the number of TRM layers, and t is the equivalent thickness of the textile in the longitudinal direction ($t = 0.095$ mm).

Table 3, lists the results of the transient condition tests including: (1) the constant load (25%, 50% or 75% of the ambient temperature strength) in which specimens were subjected; (2) the time required to reach failure for both twin specimens S1 and S2; (3) the corresponding average time for the twin specimens; (4) the temperature reached at the concrete-matrix interface at failure for twin specimens S1 and S2; (5) the corresponding average temperature; and (6) the observed failure mode.

The measurements of the strain gages at high temperatures were and not reliable and therefore are not presented.

3.1. Temperature profile

Fig. 8 presents a typical temperature- time curve obtained from the two thermocouples affixed at the concrete- matrix interface, for a specimen tested in steady state condition and heated up to

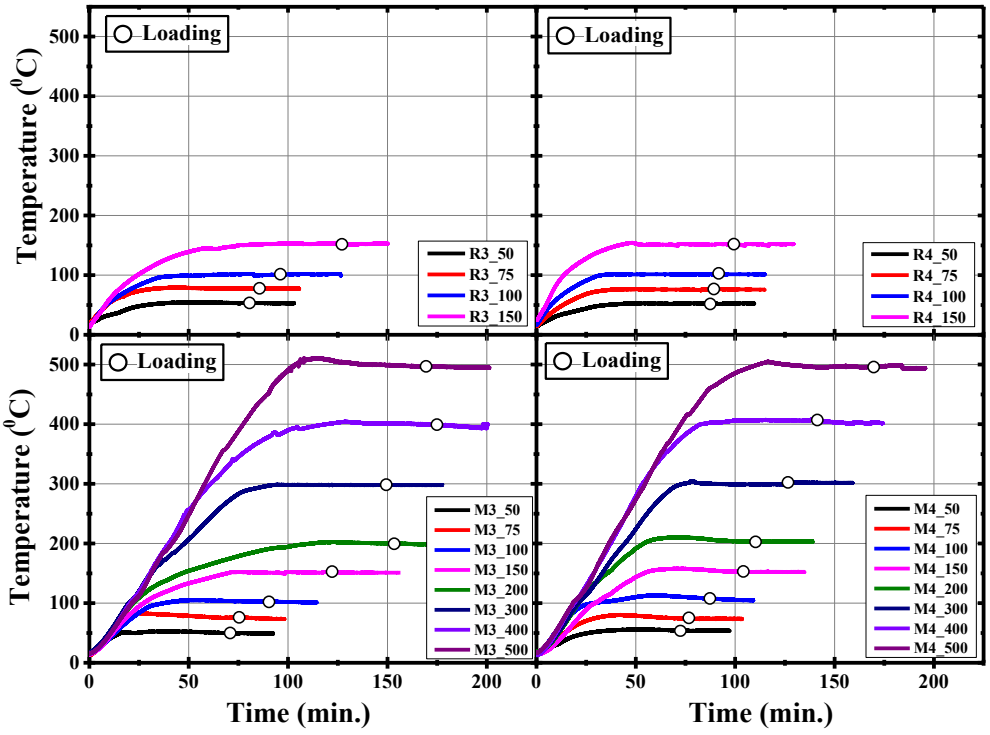

Fig. 9. Actual time- temperature curve of the specimens tested in steady state condition.

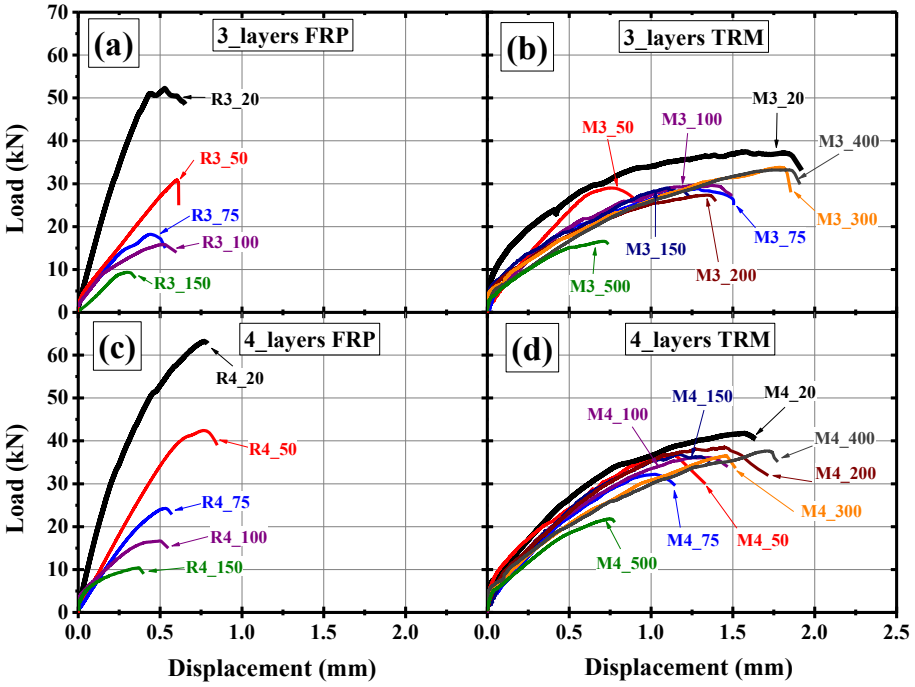

Fig. 10. Load-displacement curves of the specimens strengthened with different materials and number of layers: (a) three.

400 °C. Since the readings (in all tests) were identical, the average (of the two thermocouples) temperature was used. Fig. 9 displays the actual temperature- time curves for all FRP and TRM-strengthened specimens tested in steady state condition. It can be observed that: (a) the heating rate is identical between all specimens and (b) all specimens were exposed to predefined temperature for 1 h before application of the load, and then tested under displacement control up to failure. Note that the consistency in the heating procedure for all tested specimens is important to reduce errors, obtain reliable, and comparable measurements, and hence increase the level of confidence in the obtained results.

3.2. Load- displacement curves

Fig. 10a-d presents the load-displacement curves of all FRP/TRM strengthened specimens tested in steady-state condition. For better clarity, only one of the twin specimen's curves is presented in this figure. Moreover, they were grouped on the basis of the strengthening materials used and number of layers. Starting from FRP-retrofitted specimens (Fig. 10a and c), the load vs displacement curves were characterised by a linear ascending branch with progressive decreasing in the stiffness due to softening of the (concrete-resin) interface up to failure. On the other hand, the TRM-strengthened specimens' curves were characterized by two ascending branches. The first ascending branch was linear with high axial stiffness up to mortar cracking, followed by a nonlinear one with progressively decreasing stiffness up to failure (Fig. 10b and d).

Fig. 11a and b, depicts the increase of the crosshead displacement and the average temperature at the concrete - adhesive interface with time, for specimens strengthened with 4 FRP and TRM layers, respectively, and tested in transient condition. The initial part of the curves shows the stage of loading to reach the predefined load fractions (25%, 50%, or 75% of the ambient load);

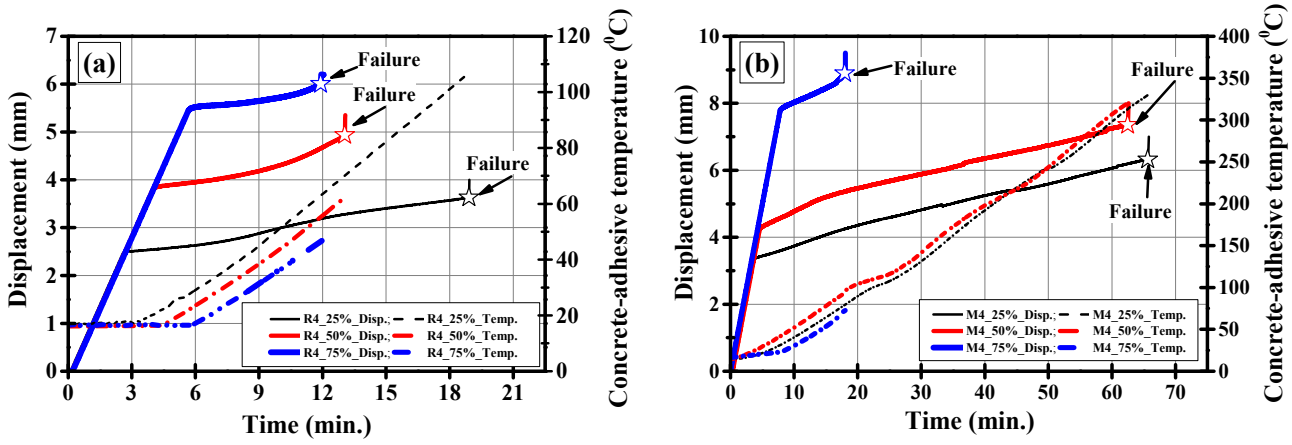

Fig. 11. Cross-head displacement increase and average temperature at the bonded interface vs. time of specimens from transient condition for specimens strengthened with (a) FRP and (b) TRM.

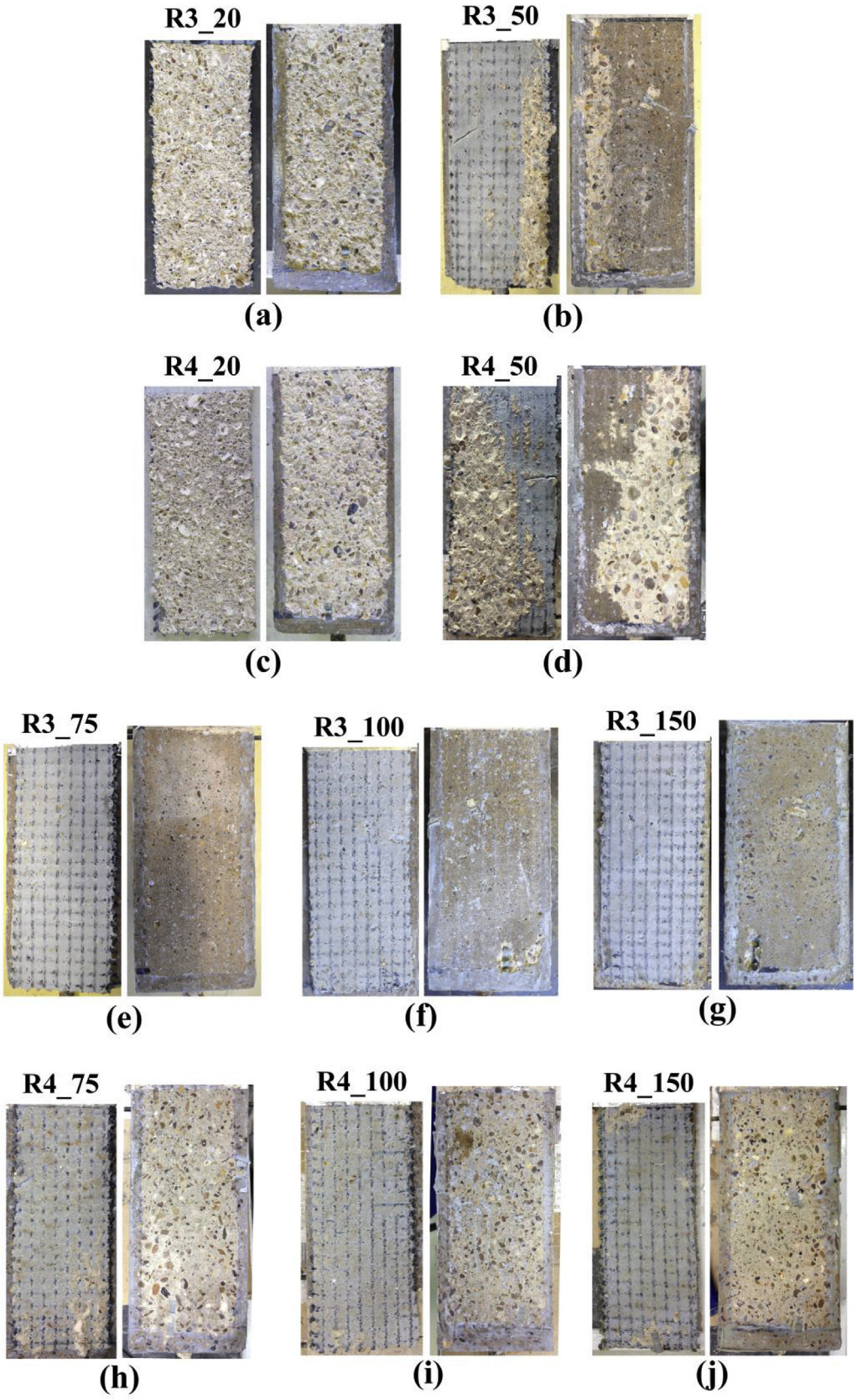

Fig. 12. Failure mode of specimens strengthened with three and four layers of FRP tested in steady state condition at different elevated temperature varied from 20 to 150 °C.

whereas the second part represents the increase of the cross-head displacement due to the heating of the specimens up to failure.

3.3. Loading condition

3.3.1. Steady state condition: ultimate load and failure mode

For the FRP retrofitted specimens, the ultimate load recorded average of two specimens was: (a) 51.3, 30.0, 17.9, 14.7, and 9.1 kN, and (b) 62.2, 40.6, 22.6, 15.8, and 9.8 kN, for the specimens strengthened with 3 and 4 layers, at the temperatures of 20, 50, 75, 100, and 150 °C, respectively. For the TRM-retrofitted specimens the ultimate load attained was equal to: (a) 36.0, 29.3, 26.5, 29.4, 30.9, 26.2, 35.9, 35.4, and 17.9 kN; and (b) 41.5, 34.0, 34.4, 36.2, 36.5, 36.9, 38.9, 39.2, and 23.1 kN (average of two specimens) for specimens reinforced with 3 and 4 layers of TRM and testes at ambient, 50, 75, 100, 150, 200, 300, 400, and 500 °C, respectively (see

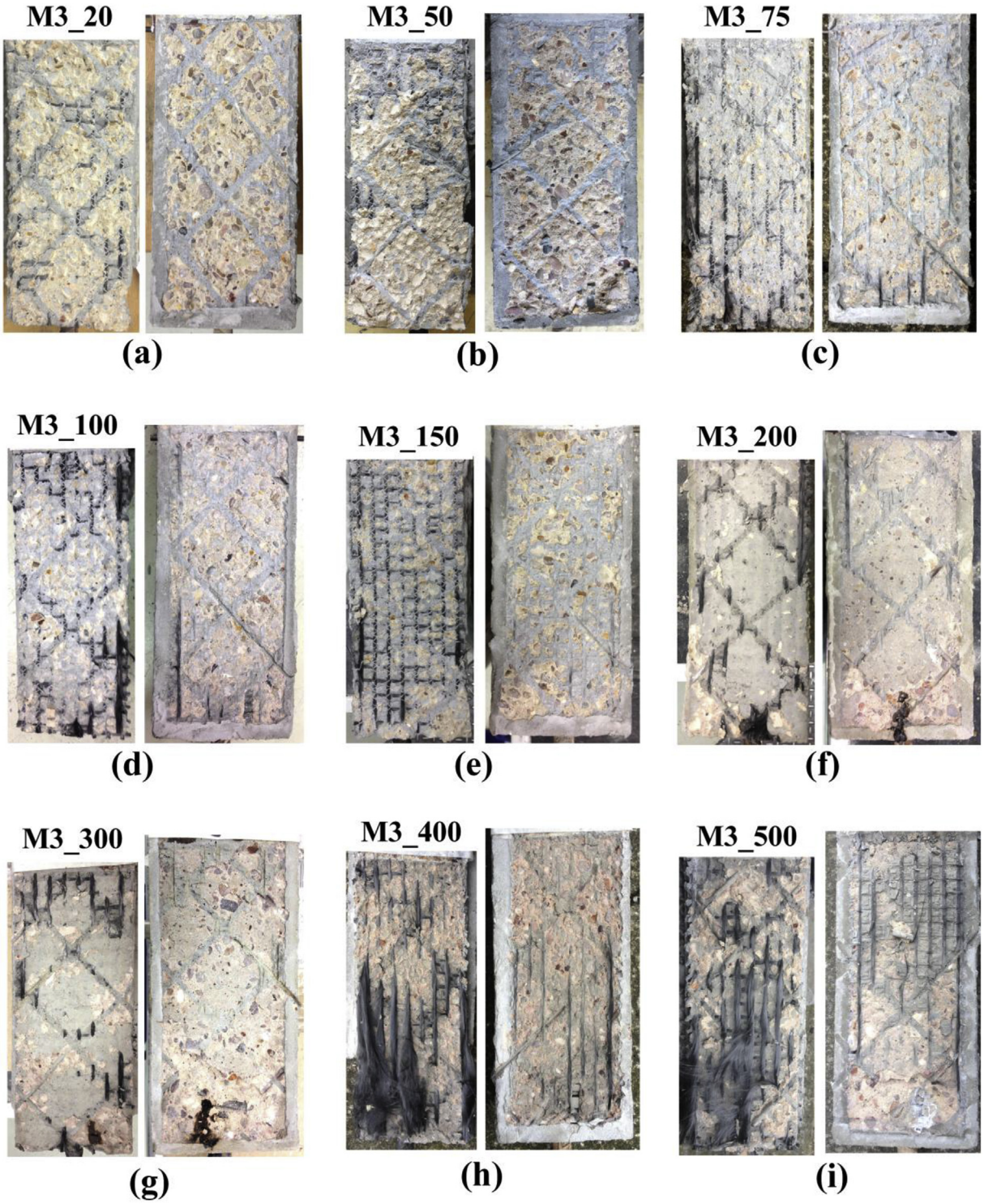

Fig. 13. Failure mode of specimens strengthened with three layers of TRM tested in steady state condition at different elevated temperature varied from 20 to 500 °C.

Table 2).

Two types of failure modes were observed for FRP-strengthened specimens: (a) deboning of FRP from the concrete substrate including parts of the concrete cover being peeled off (Fig. 12a–d), and (b) adhesive failures at the concrete- resin interface (Fig. 12e–j). The first failure mode occurred in all FRP-strengthened specimens tested at 20 °C and 50 °C. On the other hand, when the temperature increased to 75, 100 and 150 °C, adhesive failure at the concrete-resin interface occurred for all specimens, due to the poor bond behaviour of epoxy resin at temperature above the T_g. On the contrary, for all TRM-retrofitted specimens, regardless of the number of layers, the only observed failure mode was debonding of TRM from the concrete substrate accompanied with parts of concrete cover (Fig. 13a–i, and Fig. 14a–i).

3.3.2. Transient test: time, temperature at failure, and failure mode

As reported in Table 3, the average time and temperature at failure for FRP- reinforced specimens were: 19.0 min, 17.0 min, and 12.3 min and 96.3 °C, 70.7 °C, and 48.9 °C, respectively, for specimens loaded up to 25%, 50%, and 75% of their ambient bond strength. The corresponding values of TRM- retrofitted specimens (M4_25%, M4_50%, and M4_75%) were significantly higher namely, 62.0 min, 58.8 min, and 19.5 min and 319.5 °C, 310.4 °C, and 77.3 °C.

Adhesive failure at the concrete- resin interface (Fig. 15a) was

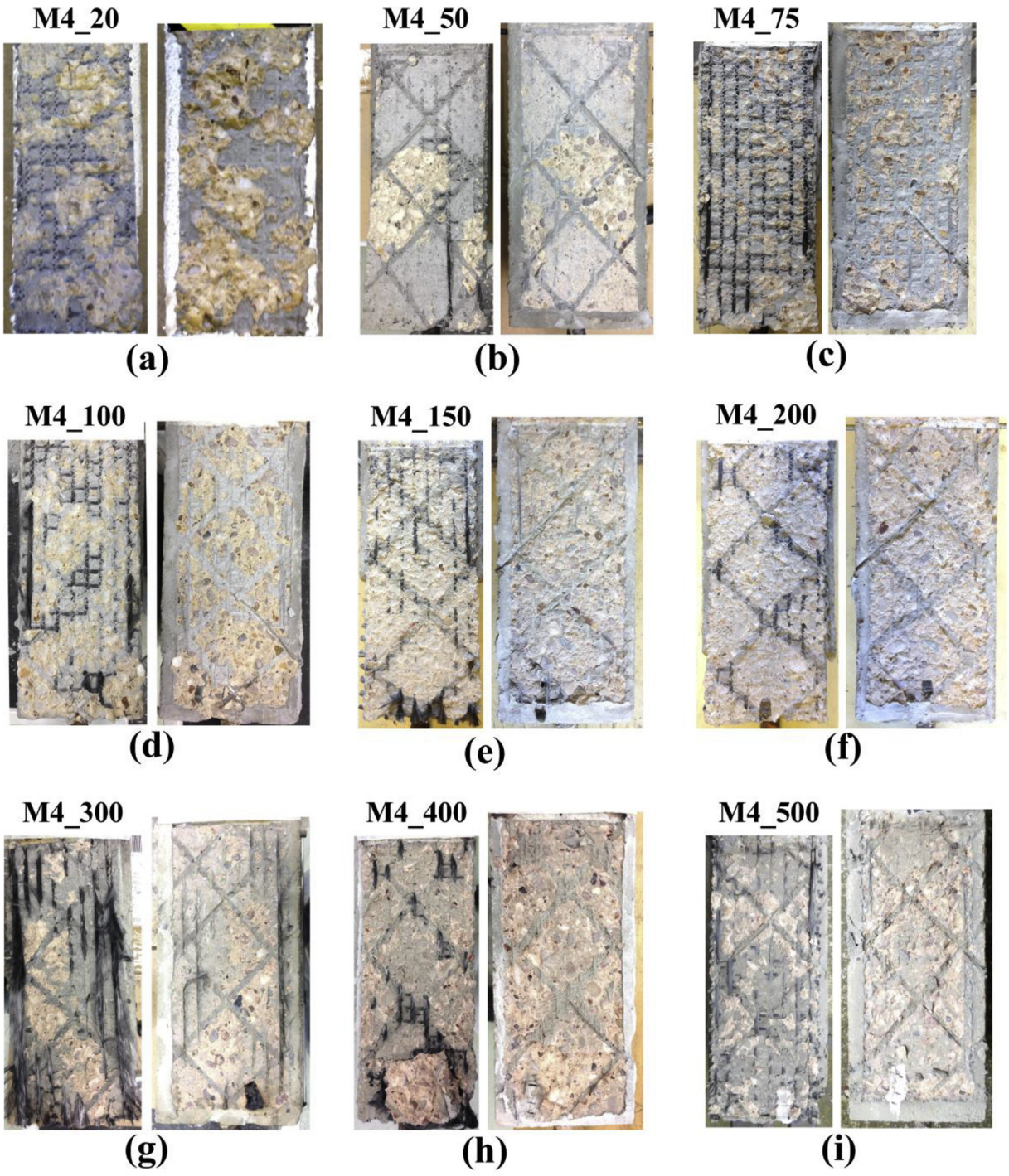

Fig. 14. Failure mode of specimens strengthened with four layers of TRM tested in steady state condition at different elevated temperature varied from 20 to 500 °C.

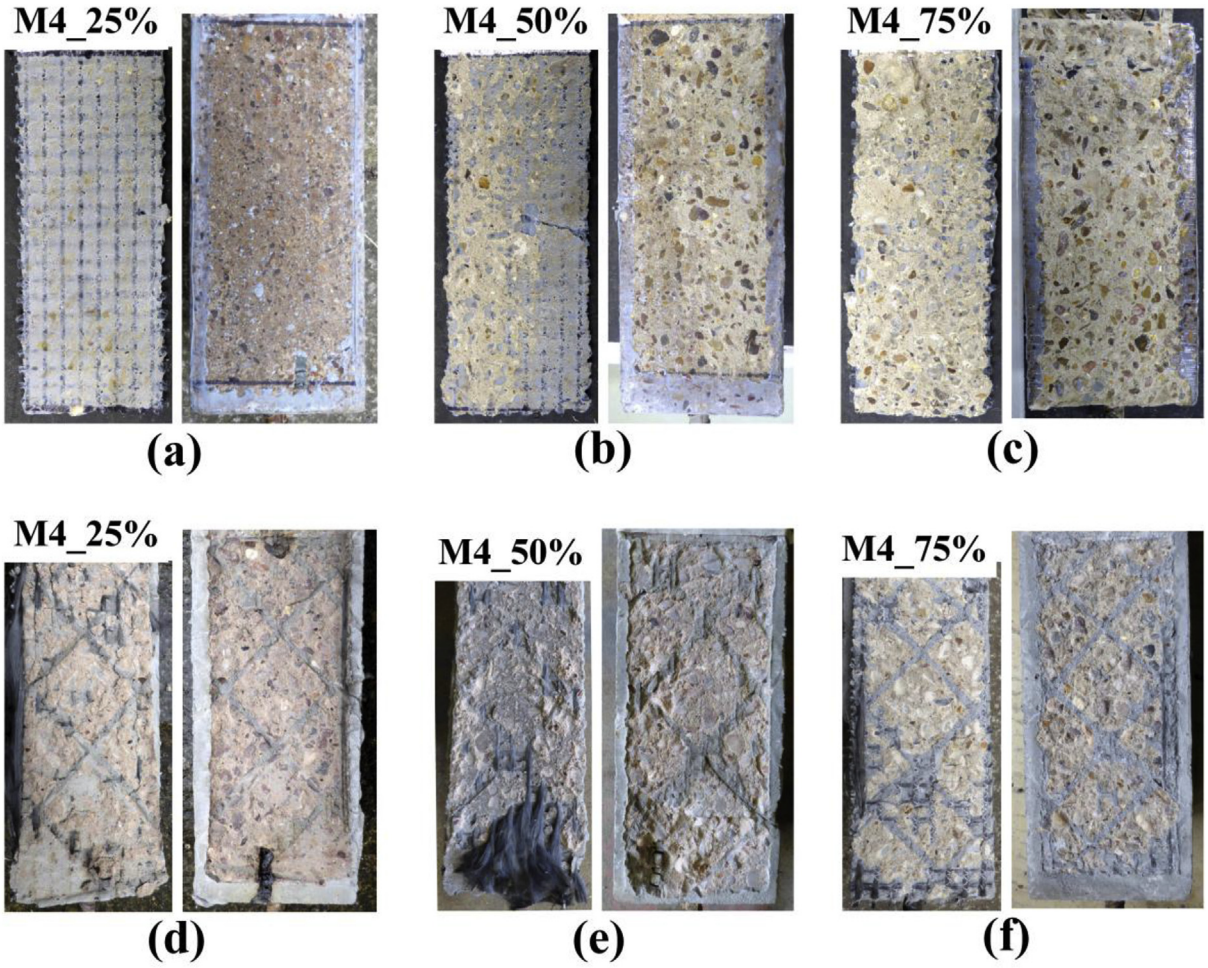

Fig. 15. Failure mode of specimens tested in transient condition.

observed for FRP-strengthened specimens subjected to the low load fraction (R4_25%). Whereas debonding of FRP from the concrete substrate with including parts of concrete cover (Fig. 15b and c) was noted for the moderate and high load fractions (R4_50%, and R4_75%). These failure modes were essentially related to temperature developed at the interface at the onset of failure, namely debonding and adhesive failures for temperatures below and above the T_g, respectively. For TRM strengthened specimens, premature adhesive failure modes were prevented due to the better resistance of mortar than resin at temperatures above T_g, with all specimens failing due to debonding including part of the concrete cover (Fig. 15d–f).

4. Discussion

In terms of the various parameters investigated in this experimental programme, an examination of the results (Tables 2 and 3) revealed the following information.

4.1. Matrix materials (TRM vs. FRP)

The matrix material (epoxy resin or mortar) significantly affects the bond performance of FRP and TRM composites with concrete at ambient and especially at high temperatures. At 20 °C, although both FRP and TRM-strengthening specimens failed due to debonding including part of concrete cover, the bond performance of FRP- strengthened specimens was considerably better than TRM ones. The bond strength of 3 and 4 layers FRP specimens was 1.4, and 1.5 times higher than that of counterpart TRM specimens respectively, (see Table 2). This is attributed to the excellent bond between FRP composite and concrete substrate which is confirmed by the amount of concrete being peeled off (see Fig. 12a and c for FRP specimens and Figs. 13a and 14a for TRM specimens). However, at high temperatures, the TRM system exhibited excellent bond performance with concrete, which was superior to that of FRP systems. In particular, in steady- state tests, the TRM specimens retained an average of 85% of their ambient bond strength up to 400 °C. On the contrary, the FRP systems maintained approximately 17% of their ambient bond strength at 150 °C due to the premature adhesive bond failure at the concrete-resin interface. In the next sections a comparison between the effectiveness of FRP vs. TRM materials at high temperatures is made in terms of the exposed temperature, the number of layers, and the loading condition.

4.2. Temperature

Fig. 16a shows the variation of the ultimate load with both the temperature and the number of layers for all specimens tested in steady-state condition. The bond of the FRP strengthening system to the concrete substrate was dramatically reduced with the temperature increase. In specific, the average bond strength was decreased by 42, 65, 71, and 82%; when the temperature increased

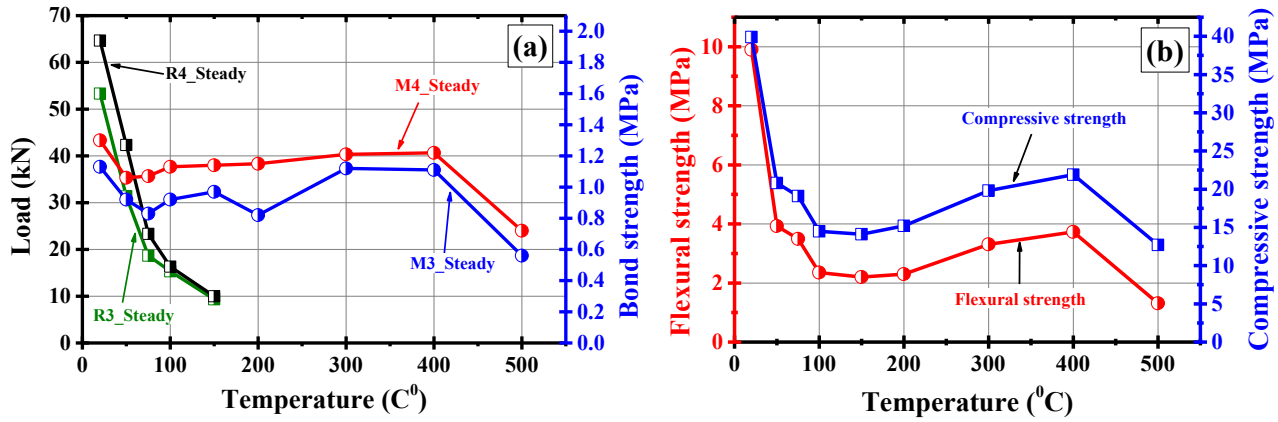

Fig. 16. (a) Variation of ultimate load and bond strength with the temperature, the strengthening materials and the number of layers (steady state tests), and (b) variation of mortar flexural and compressive strength with the temperature.

from 20 to 50, 75, 100, and 150 °C, for specimens strengthen with 3 FRP layers. The corresponding decreases in the case of 4 layers were almost identical, namely 35, 64, 75 and 84%. Similar observations were made by Firmo et al., 2015 [2], where the reductions in the bond strength were 68 and 77% when the measured temperature at the concrete-adhesive interface of FRP-strengthened specimens was 90 and 120 °C, respectively. Also, the current results, are in agreement with those of Tetta et al., 2016 [33], where the contribution of FRP U-jackets in resisting shear forces in RC strengthened beams decreased by 60 and 88% (compared to the strengthened beam tested at 20 °C) when the beams heated up to 100 and 150 °C, respectively, due an identical adhesive bond failure mode at the concrete - resin interface.

For TRM specimens, regardless the number of layers, the curves in Fig. 16a clearly demonstrate that the effectiveness of TRM in transferring the load is not significantly affected by increasing the temperature up to 400 °C. Compared to the bond strength at 20 °C, the average reduction in the bond strength was 19, 27, 18, 14, 27, 0, 2, and 50%; for the specimens subjected to temperatures of 50, 75, 100, 150, 200, 300, 400, and 500 °C, respectively, and strengthened with 3 TRM layers. The corresponding reductions for 4 TRM layers were equal to 18, 17, 13, 12, 11, 6, 6, and 44%.

A fluctuation in the bond strength was noted at temperatures varied between 50 and 200 °C, and this could be attributed to the corresponding mechanical properties of the used cement mortar. As shown in Fig. 16b, the flexural and compressive strength of the mortar considerably deteriorated, possibly due to water vapouring process which occurred at these ranges of temperatures. However, above 200 °C, an enhancement in the TRM bond strength was observed (Fig. 16a) resulting in marginal bond reductions in comparison with the ambient strength, namely equal to 3 and 4% when the temperature attained 300 and 400 °C, respectively. The highest reduction in the bond strength was 48% for TRM specimens tested at 500 °C (Fig. 16a) seems to be attributed to the reduced tensile and compressive strength of the mortar by 87% and 68% at that temperature (Fig. 16b).

The observation that the reduction of bond strength is associated with the mortar strength is better explained if someone compares the quantity of concrete being peeled off. All TRM-strengthened specimens tested at ambient and high temperature failed due to deboning, but the concrete cover detached at high temperature was thinner than the cover detached at ambient (see Fig. 13c vs. Fig. 13a), indicating the effect of the tensile strength of the mortar on the bond strength even for failure at the concrete substrate.

Finally, an attempt was made to examine the bond performance of TRM at 600 °C; however, when the interface temperature reached 550 °C, the specimen failed due to spalling of the concrete cover in an explosive manner. It is worth noting though that the TRM was still bonded to the concrete substrate even after the specimen's failure as illustrated in Fig. 17. Such a type of failure was also observed by Chowdhury et al., 2007 [35] in column tests under fire scenario.

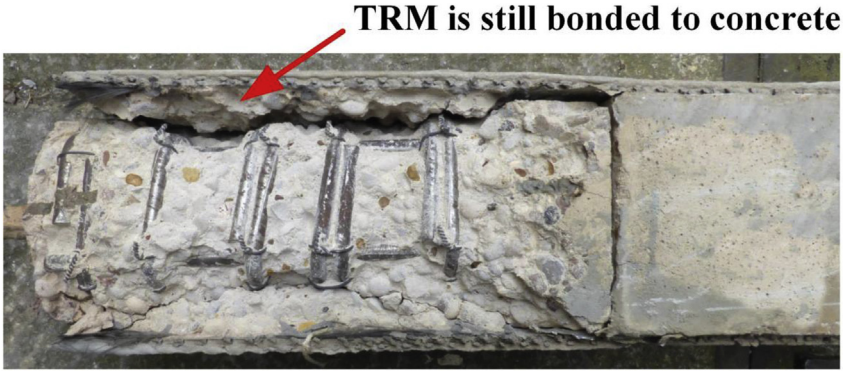

Fig. 17. Exploded specimen heated up to 550 °C.

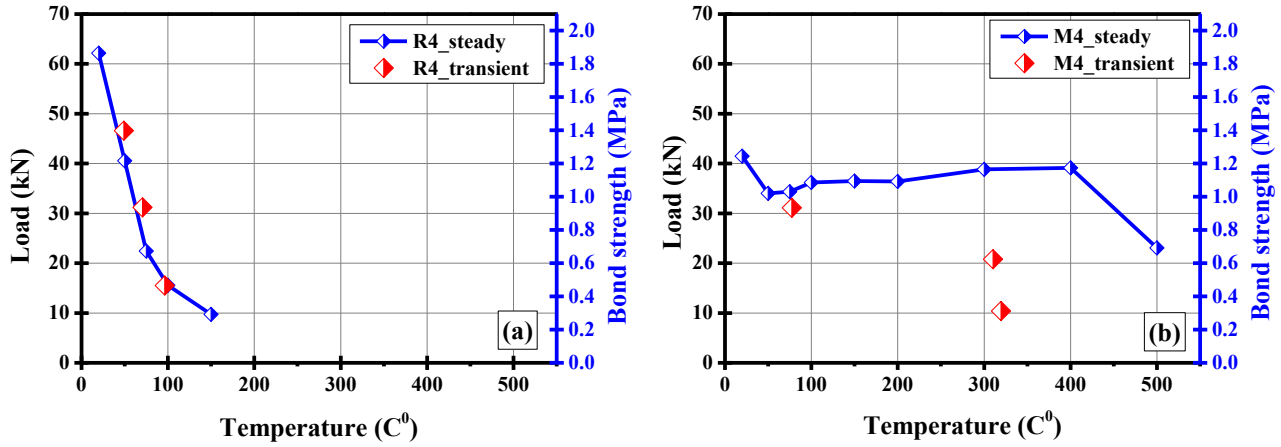

Fig. 18. Influence of the loading condition as a function of temperature on the ultimate load and bond strength of: (a) FRP-specimens, and (b) TRM specimens.

4.3. Influence of the number of layers

As depicted in Fig. 16a, when the number of layers increased from 3 to 4, the ultimate load increased by 1.21 and 1.15 for FRP and TRM specimens tested at ambient temperatures, respectively. However, at high temperatures, the influence of the number of layers on the bond strength was more pronounced for the TRM than FRP specimens. As shown in Fig. 16a, for FRP specimens, the effect of number of layers on the bond strength was almost disappeared above the T_g, as it was controlled by the properties of the epoxy resin.

The influence of the number of TRM layers on the bond strength was not that clear, with specimens receiving 4 layers having an overall higher bond strength for all temperatures investigated. It is worth mentioning that Rambo et al., 2015 [31] observed similar results in TRM coupon tensile test, in which the tensile behaviour at high temperature of TRM coupons made of 3 and 5 fabric layers was better than the tensile performance of a TRM coupon made of one layer. Tetta and Bournas. 2016 [33] concluded that by increasing from 2 to 3 TRM layers the bond of TRM to concrete at high temperatures increases considerably.

4.4. Loading conditions

As it can be observed in Fig. 18 for the transient tests, when the load fraction level was increased, the time to reach failure was decreased and consequently the temperature did, for both FRP and TRM specimens strengthened with 4 layers. Also, it is illustrated that the TRM outperformed their FRP counterparts for all load fractions. Particularly, the time required to reach failure of the TRM specimens was 3.3, 3.5 and 1.58 times higher for the low, moderate and high load fractions, respectively. Correspondingly, the attained temperature at failure was 3.3, 4,4 and 1.58 higher in the TRM-strengthened prisms.

Another interesting observation from Fig. 18a is that the bond strength attained at different temperatures was nearly identical for both loading conditions for the FRP-strengthened specimens. This confirmed that the temperature at the concrete- resin interface controlled the bond behaviour rather than the loading condition, as also reported by Firmo et al., 2015 [2]. This was not the case for the TRM system which was sensitive to the loading conditions. In fact, the TRM specimens had increased bond strengths at higher temperatures in the steady state in respect with the transient tests. As illustrated in Fig. 18b, the measured bond strength of M4_300 which was subjected to 300 °C, was almost double and triple the predefined bond strengths of specimens M4_50% and M4_25%, respectively which failed at around 300 °C.

5. Conclusions

This paper investigates the bond between TRM vs. FRP and concrete substrates at high temperatures for the first time. The investigated parameters included the strengthening system (TRM vs FRP), the exposure temperature, the number of FRP/TRM layers, and the loading conditions. For this purpose, 68 specimens were constructed, strengthened, and tested under double-lap direct shear at ambient and high temperatures. The main findings of the current study are summarized below:

1. The bond between the TRM strengthening system and concrete substrate remains excellent at high temperatures.
2. In steady state tests the reduction in bond strength of FRP-strengthened specimens was significantly higher than for the TRM-retrofitted specimens with the increase of the temperature. The average reduction in the bond strength of FRP-concrete interface was about 83% when the temperature reached 150 °C. Whereas the corresponding values in TRM-concrete interface was about 15% when the temperature attained 400 °C.
3. Two types of failure modes were observed in the FRP strengthened specimens tested in steady state condition. At ambient and moderate temperature (50 °C), cohesive failure was observed; in which parts of concrete cover remaining attached to the adhesive. Whereas, at elevated temperatures (i.e. 75, 100, and 150 °C), adhesive failure at the concrete-resin interface was occurred. On the other hand, for TRM specimens subjected to temperatures (up to 500 °C), the failure was due to TRM debonding with parts of concrete cover peeling off.
4. The bond strength at the FRP-concrete interface was nearly identical for the same temperature regardless of the loading condition (transient or steady state). On the contrary, the bond behaviour at the TRM-concrete substrate was sensitive to the loading condition, and resulted to considerably higher bond strengths (for nearly the same temperature) in the steady state in respect with the transient tests.

Further research is required to investigate the bond between TRM made of different types of textile fibres materials and concrete at high temperature.

Acknowledgments

This work was supported by the Engineering and Physical

Sciences Research Council [grant number EP/L50502X/1] UK, and the research described in this paper has been co-financed by the Higher Committee for Education Development in Iraq (HCED).

References

[1] Kodur VKR, Bisby LA, Green M. Experimental evaluation of the fire behaviour of insulated fibre-reinforced-polymer-strengthened reinforced concrete columns. Fire Saf J 2006;41(7):547–57.

[2] Firmo JP, Correia JR, Bisby LA. Fire behaviour of FRP-strengthened reinforced concrete structural elements: a state-of-the-art review. Compos Part B Eng 2015;31(80):198–216.

[3] Bournas DA, Lontou PV, Papanicolaou CG, Triantafillou TC. Textile-reinforced mortar versus fiber-reinforced polymer confinement in reinforced concrete columns. ACI Struct J 2007;104(6).

[4] Brameshuber W. State-of-the-art report of RILEM technical committee 201 TRC: textile reinforced concrete (RILEM report 36). Bagneux: RILEM Publications SARL; 2006.

[5] Carloni C, Bournas DA, Carozzi FG, D'Antino T, Fava G, Focacci F, et al. Fiber reinforced composites with cementitious (inorganic) matrix [Chapter 9]. In: Pellegrino C, Sena-Cruz J, editors. Design procedures for the use of composites in strengthening of reinforced concrete structures – state of the art report of the RILEM TC 234-DUC. Springer, RILEM STAR Book Series; 2015. p. 349–91.

[6] Ombres L. Flexural analysis of reinforced concrete beams strengthened with a cement based high strength composite material. J Comps Struct 2011;94:143–55.

[7] D'Ambrisi A, Focacci F. Flexural strengthening of RC beams with cement-based composites. J Compos Constr ASCE 2011;15(5):707–20.

[8] Ebead U, Shrestha KC, Afzal MS, El Refai A, Nanni A. Effectiveness of fabric-reinforced cementitious matrix in strengthening reinforced concrete beams. J Compos Constr ASCE 2016:1–14. http://dx.doi.org/10.1061/(ASCE)CC.1943-5614.0000741.

[9] Raoof SM, Koutas LN, Bournas DA. Textile-Reinforced Mortar (TRM) versus Fiber-Reinforced Polymers (FRP) in Flexural strengthening of RC beams. J Constr build mats 2017. http://dx.doi.org/10.1016/j.conbuildmat.2017.05.023.

[10] Schladitz F, Frenzel M, Ehlig D, Curbach M. Bending load capacity of reinforced concrete slabs strengthened with textile reinforced concrete. Eng structs 2012;40:317–26.

[11] Loreto G, Leardini L, Arboleda D, Nanni A. Performance of RC slab-type elements strengthened with fabric-reinforced cementitious-matrix composites. J Comps Constr 2013;18(3). A4013003:1–9.

[12] Koutas LN, Bournas DA. Flexural strengthening of two-way RC slabs with textile reinforced mortar: experimental investigation and design equations. J Compos Constr 2016;21(1). 04016065; 1–11.

[13] Tetta ZC, Koutas LN, Bournas DA. Textile-reinforced mortar (TRM) versus fiber-reinforced polymers (FRP) in shear strengthening of concrete beams. Comps Part B 2015;77:338–48.

[14] Tetta ZC, Koutas LN, Bournas DA. Shear strengthening of full-scale RC T-beams using textile-reinforced mortar and textile-based anchors. Comps Part B 2016;95:225–39.

[15] Ombres L, Verre S. Structural behaviour of fabric-reinforced cementitious matrix (FRCM) strengthened concrete columns under eccentric loading. Comps Part B 2015;75:235–49.

[16] Bournas DA, Triantafillou TC, Zygouris K, Stavropoulos F. Textile-reinforced mortar versus FRP jacketing in seismic retrofitting of RC columns with continuous or lap-spliced deformed bars. J Compos Constr 2009;13(5):360–71.

[17] Bournas DA, Triantafillou TC. Bond strength of lap-spliced bars in concrete confined with composite jackets. J Comp Constr 2011;15(2):156–67.

[18] Bournas DA, Triantafillou TC. Bar Buckling in RC Columns confined with composite materials. ASCE J Compos Constr 2011;15(3):393–403.

[19] Bournas DA, Triantafillou TC. Biaxial bending of RC columns strengthened with externally applied reinforcement combined with confinement. ACI Struct J 2013;110(2):193–204.

[20] Bournas DA, Pavese A, Tizani W. Tensile capacity of FRP anchors in connecting FRP and TRM sheets to concrete. Eng Structs 2015;82:72–81.

[21] Koutas L, Bousias SN, Triantafillou TC. Seismic strengthening of masonry-infilled RC frames with TRM: experimental study. J Comp Constr 2015;19(2):04014048. http://dx.doi.org/10.1061/(ASCE)CC.1943-5614.0000507.

[22] Gamage JC, Wong MB, Al-Mahaidi R. Performance of CFRP strengthened concrete members under elevated temperatures. In: Proceedings of the international symposium on bond behaviour of FRP in structures; 2005. p. 113–8.

[23] Klamer EL, Hordijk DA, Janssen HJ. The influence of temperature on the debonding of externally bonded CFRP. Special issue ACI 2005;230:1551–70.

[24] Leone M, Matthys S, Aiello MA. Effect of elevated service temperature on bond between FRP EBR systems and concrete. Compos Part B Eng 2009;40(1):85–93. 31.

[25] Firmo JP, Correia JR, Pitta D, Tiago C, Arruda MRT. Experimental characterization of the bond between externally bonded reinforcement (EBR) CFRP strips and concrete at elevated temperatures. Cem Concr compos 2015;60:44–54.

[26] D'Ambrisi A, Feo L, Focacci F. Experimental analysis on bond between PBO-FRCM strengthening materials and concrete. Compos Part B 2013;44(1):524–32.

[27] D'Antino T, Pellegrino C, Carloni C, Sneed LH, Giacomin G. Experimental analysis of the bond behavior of glass, carbon, and steel FRCM composites. In Key Eng Mat.

[28] Raoof SM, Koutas LN, Bournas DA. Bond between Textile-Reinforced Mortar (TRM) and concrete substrates: experimental investigation. Comps Part B 2016;98:350–61.

[29] Colombo I, Colombo M, Magri A, Zani G, di Prisco M. Textile reinforced mortar at high temperatures. In: Applied mechanics and materials, vol 82. Trans Tech Publications; 2011. p. 202–7.

[30] de Andrade Silva F, Butler M, Hempel S, Toledo Filho RD, Mechtcherine V. Effects of elevated temperatures on the interface properties of carbon textile-reinforced concrete. Cem Concr Compos 2014;30(48):26–34.

[31] Rambo DA, de Andrade Silva F, Toledo Filho RD, Gomes OD. Effect of elevated temperatures on the mechanical behavior of basalt textile reinforced refractory concrete. Mater Des 2015;31(65):24–33.

[32] Bisby L, Stratford T, Hart C, Farren S. Fire performance of well-anchored TRM, FRCM, and FRP flexural strengthening systems. ACIC 2013 Adv Compos Constr 2013.

[33] Tetta ZC, Bournas DA. TRM vs FRP jacketing in shear strengthening of concrete members subjected to high temperatures. Compos Part B Eng 2016;1(106):190–205. http://dx.doi.org/10.1016/j.compositesb.2016.09.026.

[34] 1015-11 EN. Methods of test for mortar for masonry – Part 11: determination of flexural and Compressive strength of hardened mortar. Brussels: Comité Européen de Normalisation; 1993.

[35] Chowdhurya EU, Bisby LA, Green MF, Kodurb VKR. Investigation of insulated FRP-wrapped reinforced concrete columns in fire. Fire Saf J 2007;42(6):452–60.